To appear in *Advanced Robotics*
Vol. 30, No. 20, July 2016, 1–13

**Regular Paper**

# *Walk control of segmented multi-legged robot based on integrative control of legs and 2-DoF active intersegment joints*

Ryo Takahashi[a] and Shinkichi Inagaki[a]*

[a] *Graduate School of Engineering, Nagoya University, Nagoya, Japan*

(*v1.0 released January 2013*)

This paper proposes a novel walk control method for multi-legged robots which have segmented bodies like a millipede. The segment of the robot which is addressed in this paper has a pair of legs which has 3 degrees of freedom (DoF) and 2-DoF active joint which connects the adjacent segmented body. The legs are controlled based on a decentralised control method, Follow-the-Contact Point (FCP) gait control, in which the legs contact on the contact-points where the forward legs have done. The joints between segments are controlled so as to make the bodies follow a desired trajectory. The legs and the intersegment joints are controlled with integrative and consistent manner thanks to local coordinate systems defined on each contact point. Finally, the proposed control method is verified via a robot simulator with physics engine.

**Keywords:** segmented multi-legged robot; decentralised control; FCP gait control; active intersegment joint; contact-point coordinate system.

## 1. Introduction

Multi-legged robots have been earnestly studied with expecting their high mobility capability. Segmentation of the body can give the multi-legged robot versatility of its movement and scalability of its configuration. Segmented multi-legged robots look like a myriapod, like a centipede and a millipede, and are therefore possible to increase the number of legs by adding segments thanks to the homogeneous configuration.

In order to realize the segmented multi-legged robot, one of the greatest challenging points is to develop the control method to govern the redundant and massive number of degrees of freedom (DoF). Generally, there are two approaches to develop the control strategy. One is to actively control the legs and passively move the intersegment joints which are the joints connecting continuous two segmented bodies. The legs are controlled in specific patterns [1, 2] or in decentralised control manners, like central pattern generator (CPG) [3, 4] and event driven control [5, 6]. The passive intersegment joints move so as to absorb the force which is exerted to the bodies by the legs' movement. As the results, the legs and intersegment joints behave harmoniously, and the robot can walk on flat terrain [1, 2, 4, 5] and uneven terrain [6].

The other approach for controlling the segmented multi-legged robots is to control both the legs and the intersegment joints actively. The integrative control of legs and intersegment joints enhance the mobility capability of the robot. M. Sfakiotakis et al. [7] developed a polychaete-like robot whose segment has a set of 1-DoF legs like a blade and a 1-DoF intersegment joint, in which the intersegment joints are controlled so as to generate tail-to-head wave pattern with moving

*Corresponding author. Email: inagaki@nuem.nagoya-u.ac.jp

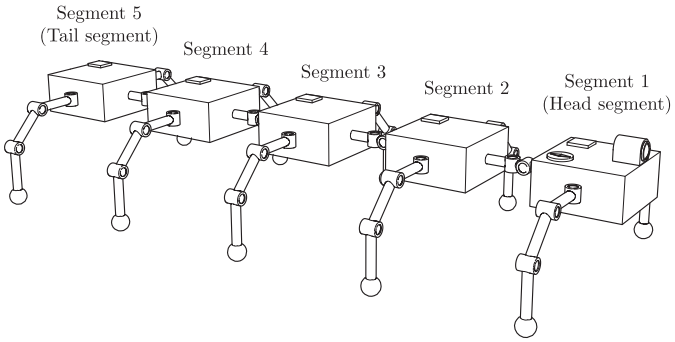


Figure 1. segmented multi-legged robot which composed of 5 segments

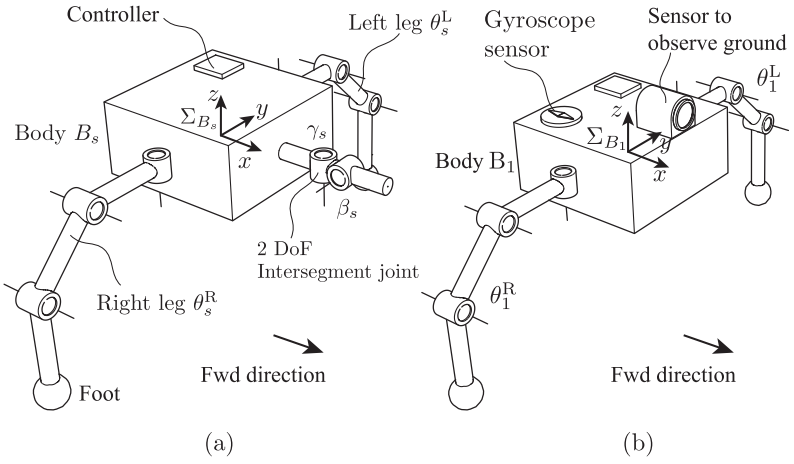


Figure 2. Segments; intermediate one ($s \neq 1$) (a), and head one ($s = 1$) (b)

the legs in phase. L. Matthey et al. [8] proposed CPG based decentralised control for a centipede-like robot whose segment has a set of 1-DoF rotating legs and a 2-DoF intersegment joint, one DoF is active in the yaw axis and the other is passive in pitch axis. They showed the robot was capable to walk on uneven terrain by simulation with physics engine. G. Long et al. [9] developed a robot whose segment has a 1-DoF circular leg and a 2-DoF active intersegment joint. The legs are mechanically linked so as to generate a millipede-like gait and the intersegment joints can be controlled to fit the segments to the contour of terrain and to lift up the head segment. T. Wei et al. [10] developed a robot whose segment has a pair of 5-DoF legs and a 2-DoF active intersegment joint, in which each joint is controlled in decentralised algorithm that generates periodic motion with delay between adjacent segments.

This paper proposes a novel integrative control for legs and intersegment joints of a segmented multi-legged robot. The segment has a pair of 3-DoF legs and a 2-DoF active intersegment joint as shown in Fig. 1. The legs are controlled based on a decentralised control, Follow-the-Contact-Point (FCP) gait control [6] in which each foot contacts on the footprint of the forward foot. The intersegment joints are controlled so that the segmented bodies follow a desired trajectory. Introducing a local coordinate system on each contact point and the transformation matrices defined on it, the legs and the intersegment joints are controlled by integrative and consistent manner. The proposed control method is verified by a simulation with physics engine.

The remaining part of this paper is organized as follows: In Sec. 2, the configuration of segmented multi-legged robot is introduced, and FCP gait control and some additional assumptions to derive the local coordinate systems on the contact points are explained. In Sec. 3, the local coordinate systems on the contact points are introduced and the integrative control of legs and intersegment joints are derived. In Sec. 4, the proposed method is experimented via a robot

simulation, and this paper is concluded in Sec. 5.

## 2. Segmented multi-legged robot

### 2.1 *Configuration of segment*

The robot which is addressed in this paper is composed of $S$ ($\geq 3$) decentralised segments as shown in Fig. 1. Each segment has a body, a pair of legs, and an intersegment joint which connects the forward adjacent body except the head segment (Fig. 2). The intersegment joint has two DoF of pitch and yaw rotational directions. Each leg has three DoFs which can move the foot to an arbitrary point in the movable area. In this paper, the foot is dealt as a point. Therefore, the foot is supposed to contact on a point of the ground. The point where the foot contacts on the ground is called 'contact point (CP)'.

The angular values of the right and left legs of segment $s \in \{1, \cdots, S\}$ are represented as vectors as $\theta_s^{\mathrm{R}}$ and $\theta_s^{\mathrm{L}}$ respectively. The pitch and yaw angular values of the intersegment joint of segment $s$ are represented as $\beta_s$ and $\gamma_s$ respectively. The leg joints and intersegment joint are driven by servomotors which are controlled based on angular control. That is, the motors are controlled to exert torque so that the joint angle converges to a target value. The target values are represented as $\theta_s^{\mathrm{R}*}$, $\theta_s^{\mathrm{L}*}$, $\beta_s^*$, and $\gamma_s^*$, respectively.

The angular values, $\theta_s^{\mathrm{R}}$, $\theta_s^{\mathrm{L}}$, $\beta_s$, and $\gamma_s$, are controlled by a controller which is allocated to each segment $s \in \{3, \cdots, S\}$. The head and second segments ($s = 1,\ 2$) are controlled in a manner different from the other ones since the target angular values of the intersegment joint between head and second segments are exceptionally derived based on a gyroscope sensor equipped on the head segment. The details are explained in Sec. 3.

As shown in Fig. 3, the bodies are labelled as $B_s$ ($s = 1, 2, \cdots, S$) from the head to tail segments. The CPs are numbered as $C_i$ ($i = 1, 2, \cdots$) toward the forward direction and alternately from left to right. Then, the set of CPs is represented as $\mathbf{C} = \{C_1, C_2, \cdots\}$. The CPs should be planned with the robot moving in real time, but in this paper, the CPs are given preliminary for simplicity. For example, the real time planning of CPs of a segmented multi-legged robot is proposed in [15].

The set of CPs which are contacted by the legs of segment $s$ are represented $C(s,t) \subset \mathbf{C}$. In addition, a function which extracts the index numbers from a set of CPs is defined as follows:

$$f : 2^{\mathbf{C}} \to \{1, 2, \ldots\} \tag{1}$$

where $2^A$ is the power set of $A$. For example, $f(\{C_1, C_2, C_3\}) = \{1, 2, 3\}$. Because each segment has two legs, the following condition is satisfied for all $s \in \{1, \cdots, S\}$:

$$0 \leq \#(f(C(s,t))) \leq 2, \tag{2}$$

where $\#(A)$ is the number of elements of set $A$.

### 2.2 *Control of legs: Follow-the-Contact-Point (FCP) gait control*

The FCP gait control [6] is a decentralised walk control for multi-legged robots and is one realization of Follow-The-Leader (FTL) gait strategy [11–13] realized by the form of decentralised and event-driven control architecture. In the FTL gait strategy, each foot except ones of the head segment contacts on the CP on which the forward foot has contacted. Therefore, the CPs on which the legs of head segment have contacted are inherited by the following posterior feet. Since planning the CPs of the entire legs is concentrated only in planning the CPs on which the legs of head segment will contact, the computational burden in the motion planning of the robot can be greatly decreased. Each leg has an event-driven controller represented by an automaton

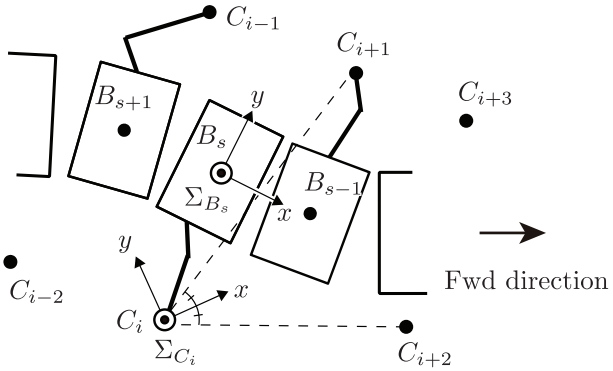


Figure 3. Definition of local coordinates of legs and segments

as shown in Fig. 4, in which the leg is operated based on the state of own leg and ones of the adjacent legs. Each state of the automaton represents a control mode which has different target points of foot $\mathbf{x}_c^*$, $c \in \{1, 2, 3, 4\}$. Then, the target angular values $\theta_s^{d*}$, $d \in \{\mathrm{R}, \mathrm{L}\}$, is calculated based on inverse kinematics of leg as follows:

$$\theta_s^{d*} = K^{-1}\left(\mathbf{x}_c^*\right) \tag{3}$$

where $K^{-1} : \mathbb{R}^3 \to \mathbb{R}^3$ is the inverse kinematics to derive the angular values to satisfy the give foot position.

The FCP gait control is composed of four control modes. Each control mode is summarised as follows, see Figs. 4 and 5 for the details:

**Control mode 1** (Swing phase 1) The foot leaves the ground and moves to a midair point $P_{up}$ $(= \mathbf{x}_1^*)$ which is represented in the local coordinate system whose origin is allocated on the middle of body. The mode transits to mode 2 when the foot reaches at $P_{up}$;

**Control mode 2** (Swing phase 2) The foot stays at $P_{up}$ $(= \mathbf{x}_2^*)$ until a new CP enters the reachable area of the own foot. The new CP is the foot position of the forward leg as for the intermediate segments $(s = 2, \cdots, S)$ and is the point which is located in just front of the body as for the head module $(s = 1)$. When the new CP enters the reachable area, the mode transits to mode 3;

**Control mode 3** (Swing phase 3) The foot goes down toward the new CP position $(= \mathbf{x}_3^*)$. The mode transits to mode 4 when the foot contacts on the new CP;

**Control mode 4** (Stance phase) The leg is controlled to keep the foot on the CP. The target point of foot $\mathbf{x}_4^*$ is derived so that the body tracks the desired trajectory. When the rear and contralateral legs are both in stance phase, the mode transits to mode 1.

In the original FCP gait control [6], $\mathbf{x}_4^*$ is calculated so as to follow a predefined line without considering the consistency of the movements among legs and bodies. In this paper, $\mathbf{x}_4^*$ is derived with considering the consistency. The details are explained in Sec. 3.3.

Each leg of the robot is assumed to be controlled by the FCP gait control thereafter. Additionally, the following conditions are assumed to be satisfied:

**Assumption 1.** *The continuous two feet contact on a same CP at the same time when they exchange the CP, and the position of foot never moves in the stance phase;*

**Assumption 2.** *The right and/or left legs of each segment always contact on the ground* :

$$\#(f(C(s,t))) \geq 1, \ \forall s \in \{1, \cdots, S\}, \forall t \ \in R^+; \tag{4}$$

**Assumption 3.** *All the CPs between the CPs on which the legs of head segment contact and*

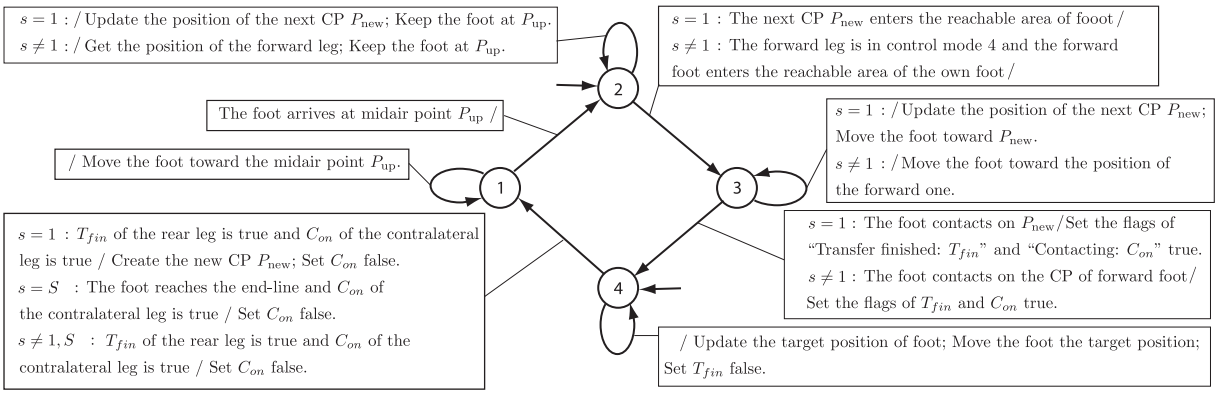


Figure 4. Automaton of FCP gait control equipped in each leg of multi-legged robot: This figure is revised from [6]; The state transition is represented like inEvent/outEvent1;outEvent2;$\cdots$. When the inEvent is true, the state transits with executing the outEvents.

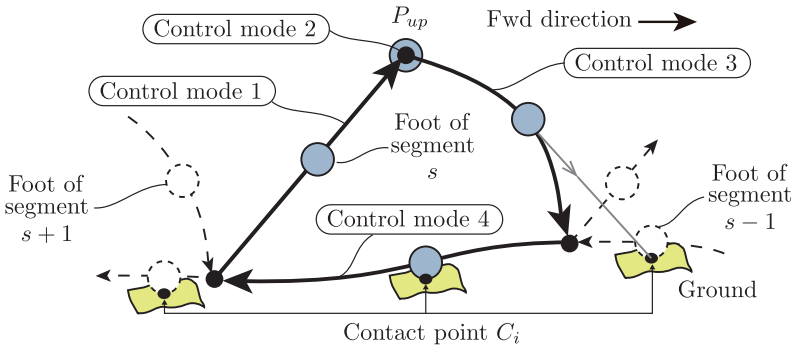


Figure 5. Foot trajectory and corresponding control modes

*the CPs on which the legs of tail segment contact are contacted by one or some legs of the robot:*

$$C_i \in \bigcup_{s=1}^{S} C(s,t),\ \forall i \in [\min f(C(S,t)), \max f(C(1,t))]\,; \tag{5}$$

**Assumption 4.** *Consecutively labelled three CPs are not on a line;*

**Assumption 5.** *The head and second segments can track at least two CPs ahead on which the legs of head segment are going to contact.*

The assumption 1 would be realized if the legs and the intersegment joints are controlled consistently and if the feet have enough strong friction force with the ground. From the assumption 1, a local coordinate system can be defined on each CP regardless of the manner that the legs contact on it. Then, the desired trajectory of the bodies is defined on each CP-coordinate system, and the target angular values of joints of legs and intersegment joints are derived based on homogeneous transformations between the CP-coordinate system and the local coordinate system which is defined on the body. The assumptions 2, 3, and 4, would be realized if the CPs are planned properly. These assumptions are required to calculate the coordinate unit vectors of each CP-coordinate system from the joints' angular values. The assumption 5 is required to calculate the CP-coordinate systems defined on the CPs on which the legs of head and second segments contact, and this assumption would be realized by using a perception system which

can observe the ground and can recognise the CPs on it.

## 3. Integrated control of legs and intersegment joints

### 3.1 *Definition of local coordinate systems*

First, some mathematical expressions are defined. The local coordinate system which has the origin at point $A$ is expressed $\Sigma_A$. The unit vectors of $x$, $y$, and $z$, directions of $\Sigma_B$ which are represented by the coordinate system $\Sigma_A$ are expressed ${}^A\mathbf{e}_{Bx}$, ${}^A\mathbf{e}_{By}$, and ${}^A\mathbf{e}_{Bz}$, respectively. Then, the rotation matrix and the homogeneous transformation matrix from $\Sigma_B$ to $\Sigma_A$ are respectively given as follows:

$$ {}^A_BR = \begin{bmatrix} {}^A\mathbf{e}_{Bx} & {}^A\mathbf{e}_{By} & {}^A\mathbf{e}_{Bz} \end{bmatrix}, \tag{6} $$

$$ {}^AT_B = \begin{bmatrix} {}^A_BR & {}^AP_B \\ 0\ 0\ 0 & 1 \end{bmatrix}, \tag{7} $$

where ${}^AP_B$ is the position vector of the $\Sigma_B$'s origin represented by $\Sigma_A$.

We define local coordinate systems which have the origins at the centre of each body as $\Sigma_{B_s}$ $(s = 1, 2, \cdots, S)$. The local coordinate systems $\Sigma_{C_i}$ $(i = 1, 2, \cdots)$ whose origins are allocated at each CP $C_i$ are also defined. The relation between $\Sigma_{B_s}$ and $\Sigma_{C_i}$ is described below. **Suppose that the CP $C_i$ is contacted by a leg of segment $s$ at time $t$ hereafter.**

First, the coordinate axes of $\Sigma_{C_i}$ are defined based on the positional relations among the CPs $C_i$, $C_{i+1}$, and $C_{i+2}$ (Fig. 3). The coordinates of CPs $C_i$, $C_{i+1}$, and $C_{i+2}$ represented by $\Sigma_{B_m}$ are ${}^{B_s}P_{C_i}$, ${}^{B_s}P_{C_{i+1}}$, ${}^{B_s}P_{C_{i+2}}$, respectively. Note that, because of the assumptions 2 and 3, the segment $s(\neq 1, 2)$ can surely obtain ${}^{B_s}P_{C_{i+1}}$ and ${}^{B_s}P_{C_{i+2}}$ from at least two forward segments through the chain of homogeneous transformations from $\Sigma_{B_s}$ to the feet which are contacting on $C_{i+1}$ and $C_{i+2}$. As for the head and the second segments $(s = 1, 2)$, from the assumption 5, ${}^{B_s}P_{C_{i+1}}$ and ${}^{B_s}P_{C_{i+2}}$ are also obtained by a perception system. Then, the unit vectors of main axes of $\Sigma_{C_i}$ represented by $\Sigma_{B_s}$ are derived as follows:

$$ {}^{B_s}\mathbf{e}_{C_ix} \propto \frac{{}^{B_s}P_{C_{i+2}} - {}^{B_s}P_{C_i}}{|{}^{B_s}P_{C_{i+2}} - {}^{B_s}P_{C_i}|} + \frac{{}^{B_s}P_{C_{i+1}} - {}^{B_s}P_{C_i}}{|{}^{B_s}P_{C_{i+1}} - {}^{B_s}P_{C_i}|}, \tag{8} $$

$$ {}^{B_s}\mathbf{e}_{C_iy} \propto \frac{{}^{B_s}P_{C_{i+2}} - {}^{B_s}P_{C_i}}{|{}^{B_s}P_{C_{i+2}} - {}^{B_s}P_{C_i}|} - \frac{{}^{B_s}P_{C_{i+1}} - {}^{B_s}P_{C_i}}{|{}^{B_s}P_{C_{i+1}} - {}^{B_s}P_{C_i}|}, \tag{9} $$

$$ {}^{B_s}\mathbf{e}_{C_iz} = {}^{B_s}\mathbf{e}_{C_ix} \times {}^{B_s}\mathbf{e}_{C_iy}. \tag{10} $$

Note that ${}^{B_s}\mathbf{e}_{C_iy} \neq \mathbf{0}$ due to the assumption 4. The homogeneous transformation from $\Sigma_{B_s}$ to $\Sigma_{C_i}$ is

$$ {}^{C_i}T_{B_s} = \begin{bmatrix} {}^{C_i}_{B_s}R & {}^{C_i}P_{B_s} \\ 0\ 0\ 0 & 1 \end{bmatrix}, \tag{11} $$

where

$$ {}^{C_i}_{B_s}R = {}^{B_s}_{C_i}R^T = \begin{bmatrix} {}^{B_s}\mathbf{e}_{C_ix} & {}^{B_s}\mathbf{e}_{C_iy} & {}^{B_s}\mathbf{e}_{C_iz} \end{bmatrix}^T, \tag{12} $$

$$ {}^{C_i}P_{B_s} = -{}^{B_s}_{C_i}R^T {}^{B_s}P_{C_i}. \tag{13} $$

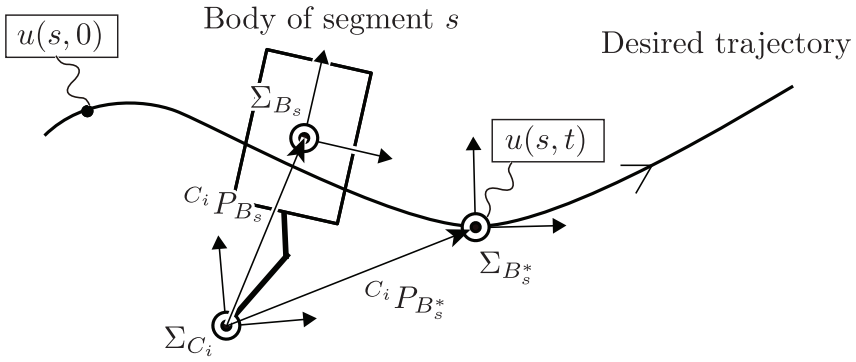


Figure 6. Desired trajectory of body segment

### 3.2 *Desired trajectory of bodies*

The legs and intersegment joint of a segment are controlled so as to follow its body along a desired trajectory which is supposed to be planned together with planning the contacting points (Fig. 6). In this paper, for simplicity, the desired trajectory is preliminarily given on the global coordinate system as follows:

$$ {}^{G}\mathbf{f}(u) = \left[{}^{G}f_x(u)\ {}^{G}f_y(u)\ {}^{G}f_z(u)\right]^T, \tag{14} $$

where $u \in \mathbb{R}$ is the parameter which indicates the location on the trajectory. In addition, in order to identify the position where the body of segment $s$ should locate on the trajectory at time $t$, a parameter $u(s,t)$ is defined as

$$ u : \{1, \cdots, S\} \times \mathbb{R}^+ \to \mathbb{R}. \tag{15} $$

For example, when the body of segment $s$ moves on the trajectory at constant speed $\delta u$, $u(s,t)$ is set as

$$ u(s,t) = u(s,0) + t\delta u, \tag{16} $$

where adequate value of $u(s,0)$ is supposed to be given to each segment $s$ based on the robot configuration at $t = 0$.

Then, the desired position where the body of segment $s$ should locate at time $t$ is represented based on the coordinate system of CP $C_i$ $(i = 1, 2, \cdots)$ as follows:

$$ {}^{C_i}P_{B_s^*} = {}^{C_i}T_G\,{}^{G}\mathbf{f}(u(s,t)) \equiv \left[{}^{C_i}f_x(u(s,t))\ {}^{C_i}f_y(u(s,t))\ {}^{C_i}f_z(u(s,t))\right]^T, \tag{17} $$

where ${}^{C_i}T_G{}^{G}$ is the homogeneous transformation from the global coordinate system to the CP-coordinate system $\Sigma_{C_i}$.

The desired trajectory should be also planned in real time together with the CPs. In [15], the desired trajectory of head segment of multi-legged robot is planned with the CPs, but the way to express the trajectory on each CP is not considered. Also, the legs are not controlled so as to follow the planned bodies' trajectory explicitly. Planning and embedding the desired trajectory on each CP in real time are one of future works.

### 3.3 *Target values of joint angles of each leg*

When a leg of segment $s$ is contacting on the CP $C_i$, the leg is operated so as to carry the body to the desired position with keeping contact on the CP. This operation is realized by setting

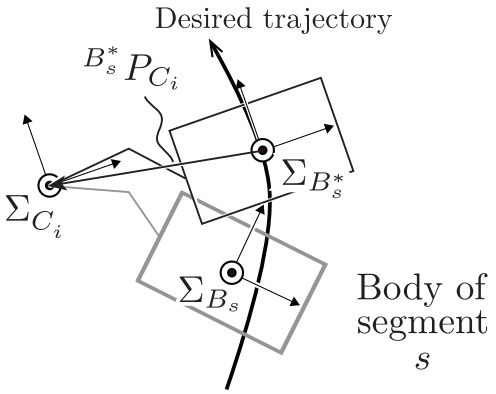


Figure 7. Contact point coordinate which is represented by the coordinate system of body

the position of the CP as the target foot position assuming the body is on the desired position (Fig. 7). The target foot position based on the coordinate system of body $B_s$ is derived as follows:

$$\mathbf{x}_4^* = {}^{B_s^*}P_{C_i} = -{}^{B_s^*}_{C_i}R\ {}^{C_i}P_{B_s^*}. \tag{18}$$

where ${}^{B_s^*}_{C_i}R$ is the rotational matrix from the CP-coordinate system $\Sigma_{C_i}$ to $\Sigma_{B_s^*}$, whose derivation is discussed in the next section.

### 3.4 *Derivation of desired body posture*

The desired posture of body is derived so that the forward direction of the body directs to the tangential direction on the desired trajectory. Therefore, the unit vector of desired forward direction is calculated based on the tangential direction of the desired trajectory at the point indicated by $u = u(s,t)$:

$${}^{C_i}e_{B_s^*x} \propto \left[\frac{d^{C_i}f_x(u)}{du}\ \frac{d^{C_i}f_y(u)}{du}\ \frac{d^{C_i}f_z(u)}{du}\right]\Big|^T_{u=u(s,t)}, \tag{19}$$

where ${}^{C_i}e_{B_s^*x}$ is the unit vector of $x$ axis of $\Sigma_{B_s^*}$ represented by the CP-coordinate system $\Sigma_{C_i}$. Using (19), the rotational matrix ${}^{B_s^*}_{C_i}R$ in (18) is calculated in different ways in the head segment ($s = 1$) and in the other segments ($s \geq 2$).

#### *3.4.1 Desired posture of the body of head segment ($m = 1$)*

The head segment is capable to perceive the globally vertical direction thanks to the gyroscope sensor equipped on its body, as shown in Fig. 2. When the unit vector of the globally vertical direction represented by the local coordinate system $\Sigma_{B_1}$ is

$${}^{B_1}e_G = \left[{}^{B_1}e_{Gx}\ {}^{B_1}e_{Gy}\ {}^{B_1}e_{Gz}\right]^T, \tag{20}$$

the tilt angle of the right and left sides of the body against the global $x$-$y$ plane is calculated as follows:

$$\theta_{\text{tilt}} = -\arctan\left(\frac{{}^{B_1}e_{Gy}}{{}^{B_1}e_{Gz}}\right). \tag{21}$$

Then, the rotational matrix to the desired posture of body $B_1^*$ represented by the coordinate

system $\Sigma_{C_i}$ is derived as

$$ {}^{B_1^*}_{C_i^*}R = {}^{B_1^*}_{B_1}R \, {}^{B_1}_{C_i^*}R \tag{22} $$

where ${}^{B_1}_{C_i^*}R$ is given by (12) and ${}^{B_1^*}_{B_1}R$ is calculated based on the roll, pitch, and yaw, angles $(\alpha_1^*, \beta_1^*, \gamma_1^*)$ from $\Sigma_{B_1}$ to $\Sigma_{B_1^*}$ as follows :

$$ {}^{B_1^*}_{B_1}R = \begin{bmatrix} \cos\gamma_1^* & \sin\gamma_1^* & 0 \\ -\sin\gamma_1^* & \cos\gamma_1^* & 0 \\ 0 & 0 & 1 \end{bmatrix} \begin{bmatrix} \cos\beta_1^* & 0 & -\sin\beta_1^* \\ 0 & 1 & 0 \\ \sin\beta_1^* & 0 & \cos\beta_1^* \end{bmatrix} \begin{bmatrix} 1 & 0 & 0 \\ 0 & \cos\alpha_1^* & \sin\alpha_1^* \\ 0 & -\sin\alpha_1^* & \cos\alpha_1^* \end{bmatrix}. \tag{23} $$

By substituting $\alpha_1^* = \theta_{\text{tilt}}$ to (23), the tilt of the body's right and left sides against the global $x$-$y$ plane disappers.

The pitch angle $\beta_1^*$ and yaw angle $\gamma_1^*$ are derived by solving the following equations:

$$ {}^{C_i}e_{B_1^*x} = {}^{C_i}_{B_1^*}R \; {}^{B_1^*}e_{B_1^*x} = {}^{B_1^*}_{C_i}R^T \; {}^{B_1^*}e_{B_1^*x}, \tag{24} $$

$$ {}^{B_1^*}e_{B_1^*x} = [1 \; 0 \; 0]^T, \tag{25} $$

so that the forward direction of the body points to ${}^{C_i}e_{B_1^*x}$. Finally, ${}^{B_1^*}_{C_1}R$ is obtained by substituting $\alpha_1^* = \theta_{\text{tilt}}$ and $\beta_1^*$, $\gamma_1^*$, which are derived by solving (24)(25), to (23).

### *3.4.2 Desired body posture except the head segment ($m \geq 2$)*

The desired postures of the intermediate and tail bodies should be derived with considering both that the forward direction of the body points to the tangential direction on the desired trajectory ${}^{C_i}e_{B_m^*x}$ and that the body $B_s$ is rotated by the intersegment 2-DOF joint which connects to the forward body $B_{s-1}$. When the relative posture between $B_s$ and $B_{s-1}$ is considered, the posture of $B_{s-1}$ is assumed to be stationary while the body $B_s$ is moving for simplicity. Under this assumption, the rotational matrix between the $B_{s-1}$ and $B_s^*$ is calculated using the target angles of the intersegment joints $\beta_s^*$ and $\gamma_s^*$ as follows:

$$ {}^{B_s^*}_{B_{s-1}}R = \begin{bmatrix} \cos\beta_s^*\cos\gamma_s^* & \sin\gamma_s^* & -\sin\beta_s^*\cos\gamma_s^* \\ -\cos\beta_s^*\sin\gamma_s^* & \cos\gamma_s^* & \sin\beta_s^*\sin\gamma_s^* \\ \sin\beta_s^* & 0 & \cos\beta_s^* \end{bmatrix}. \tag{26} $$

Then, the forward direction of desired body $B_s^*$ must coincide with the tangential direction of the desired trajectory ${}^{C_i}e_{B_s^*x}$. Therefore, the following equations are satisfied:

$$ {}^{C_i}e_{B_s^*x} = {}^{C_i}_{B_s}R \; {}^{B_s}_{B_{s-1}}R \; {}^{B_s^*}_{B_{s-1}}R^T \; {}^{B_s^*}e_{B_s^*x}, \tag{27} $$

$$ {}^{B_s^*}e_{B_s^*x} = [1 \; 0 \; 0]^T, \tag{28} $$

where ${}^{C_i}_{B_s}R$ is given by (12) and ${}^{B_s}_{B_{s-1}}R$ is calculated from the present pitch and yaw angles of the intersegment joints. Finally, using $\beta_s^*$ and $\gamma_s^*$ which are given by solving (27)(28), the desired posture ${}^{B_s^*}_{C_i}R$ is derived as follows:

$$ {}^{B_s^*}_{C_i}R = {}^{B_s^*}_{B_{s-1}}R \; {}^{B_{s-1}}_{B_s}R \; {}^{B_s}_{C_i}R. \tag{29} $$

### 3.5 *Target angular values of intersegment joints*

Each segment, except the head segment, has a 2-DOF intersegment joint which connects the own body to the forward one as shown in Fig. 2. The target angular values $\beta_m^*$ and $\gamma_m^*$ of the intersegment joint of segments $s = 3, \cdots, S$ are given by solving (27)(28) as described in the previous section. These target values are derived under the assumption that the posture of the forward body $B_{s-1}$ is stationary while the body $B_s$ is moving.

On the other hand, the target angular values $\beta_2^*$ and $\gamma_2^*$ of the intersegment joint which connects the head and the second segments are derived under the assumption that the rear body $B_2$ is stationary while the body $B_1$ is moving. Then, the rotational matrix between the $B_2$ and $B_1^*$ becomes as follows:

$$ {}^{B_1^*}_{B_2}R = \begin{bmatrix} \cos\beta_2^* \cos\gamma_2^* & \sin\gamma_2^* & -\sin\beta_2^* \cos\gamma_2^* \\ -\cos\beta_2^* \sin\gamma_2^* & \cos\gamma_2^* & \sin\beta_2^* \sin\gamma_2^* \\ \sin\beta_2^* & 0 & \cos\beta_2^* \end{bmatrix}. \tag{30} $$

Since the forward direction of $B_1$ must fit ${}^{C_i}e_{B_1^*x}$, the following equations are satisfied:

$$ {}^{C_i}e_{B_1^*x} = {}^{C_i}_{B_1}R \, {}^{B_1}_{B_2}R \, {}^{B_1^*}_{B_2}R^T \, {}^{B_1^*}e_{B_1^*x}, \tag{31} $$

where ${}^{B_1^*}_{C_i}R = \left[ {}^{C_i}e_{B_1^*x} \; {}^{C_i}e_{B_1^*y} \; {}^{C_i}e_{B_1^*z} \right]$ is derived in (22). By solving (31)(25), $\beta_2^*$ and $\gamma_2^*$ are obtained.

## 4. Experiment by physical simulation

### 4.1 *Experimental setup*

The proposed method was experimented via a robot simulator, v-rep (Virtual-Robot Experimentation Platform) [16]. We used ODE (Open Dynamics Engine) as the physics engine. Figure 8 and Table 1 respectively show the segmented multi-legged robot in the simulator and its specification. As shown in Fig. 8 (a), the segment is composed of rigid bodies; links which are drawn as cuboids; and joints drawn as cylinders. Each axis of DOF is expressed by the central axis of the cylinder. The foot is set as like a rod in order to verify that the foot keeps on a CP in the stance phase and also exchanges the CP between the adjacent legs successfully. The links between the body and the intersegment joints are not drawn merely for good visibility. The segments are connected through the intersegment joints as shown in Fig. 8 (b). The length of leg was chosen so that the reachable area of foot laps over the ones of anteroposterior feet. The weight of segment was set rather heavy and the maximum torque of the joints was set large so as to stabilise the behaviour of the robot in the simulation. The collision between legs were omitted so that the foots can contact the same point on the ground at same time.

In addition, we took countermeasure against the problem of slippage between the feet and the ground. First, the coefficient of friction between the feet and the ground was set high value. Second, a virtual spring was placed between the contacting foot and the CP which was exchanged from the front leg at the control mode 3; Note that this CP is NOT the point which is planned preliminarily. This virtual spring exerts the force only in a horizontal direction parallel to the ground and only when the foot is in the area of hemisphere whose centre is the exchanged CP. The necessity of these countermeasures is caused by the difficulty in realizing the reasonable friction force in the simulation environment. Of course, the problem of foot slippage should be carefully considered when a real robot is constructed.

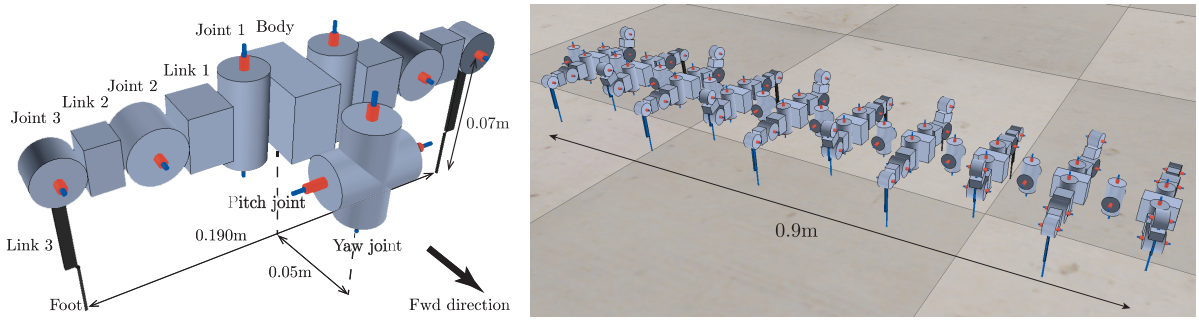


(a) Segment. (b) Robot conposed of 10 segments.

Figure 8. Segmented multi-legged robot in v-rep

Table 1. Parameters of segmented multi-legged robot in simulation environment

| | | |
|---|---|---|
| Number of segments | | 10 |
| Weight of a segment | | 30.5[kg] |
| Joint max torque | | 500[N*m] |
| Joint PID parameter | | |
| | Proportional | 1.0 |
| | Integral | 0 |
| | Derivative | 0 |
| Coefficient of friction | | 2.0 |
| Virtual spring between foot and contact point | | |
| | Effective distance | 0.03[m] |
| | Spring constant | 30000[N/m] |
| | Max force | 300[N] |

### 4.2 *Simulation results*

The simulation scenes are shown in Fig. 9 in which the robot walks on the curvilinear trajectory on a flat terrain (a) and walks over a stairs-like obstacle with maximum angle of $\pi/3$ (b). The desired trajectory which is depicted by the light blue line and the target CPs which are done by the yellow dots on the terrain were both given by a trial-and-error method preliminarily. The walk speed was given by (16) with $\delta u = 0.02$, and the proper values of $u(s, 0)$ $(s = 1, 2, \cdots, S)$ were given based on the configulation of segments. The red line and the blue line represent the real trajectories of the head segment $(s = 1)$ and the tail segment $(s = 10 = S)$ respectively. It is apparent that, more or less, each segment followed the desired trajectory in both scenes. Also, it is worth to mention that a segmented multi-legged robot whose intersegment joints were "passive" with the pure FCP gait control [6] was not able to traverse the environment of Fig. 9(b).

Figure 10 shows the position error between the body of segments $(s = 1, 5, 10)$ and the desired trajectory, the orientation error between the body orientation and the tangential direction on the desired trajectory, and the tilt angle of each body. The position error was calculated from the distance between the body position and its nearest point on the desired trajectory, and the orientation error was also derived based on the tangential direction on the nearest point. The tilt angle represent the inclination of the body's lateral direction to the horizontal plane. All these values should be zero in an ideal situation.

### 4.3 *Consideration*

Comparing (a) and (b) in Fig. 10, the position and orientation errors of the flat terrain (a) are larger than ones of the stairs-like obstacle (b). The reason is considered to be based on the difference of friction force exerted between the feet and the contact surfaces. Comparing

Figs. 9(a) and (b), the slippage of each foot from the CP which is planned preliminarily is larger in (a). The friction forces of the feet in (b) are considered to have totally worked so as to fix the feet on the CPs.

From the plots of tilt angle in Fig. 10, the tilt angle of head segment is moderated thanks to the work of gyroscope sensor. The tilt angle of tail segment is larger than one of the head segment because of the accumulation of the orientation errors from the head to tail.

From the plots of (a) in Fig. 10, the position and orientation errors increase at the values of $u$ when its body passes the points whose curvature of the desired trajectory is large. This is because the discrete structure of the chain of bodies is not able to follow the continuous curvature of the desired trajectory. In addition, especially, the orientation error of the head segment significantly become large after $u = 0.8$ because of the accumulation of foot slippage. The head segment tried to forcibly reach the feet to the contact points which were planned preliminarily. However, the feet eventually slip on the contact surface owing to the accumulation of foot slippage in the last stage of the scene. Therefore, the orientation error is considered to be enhanced in the last simulation steps.

The main advantage of the proposed method is that the segmented multi-legged robot can precisely follow the target trajectory and CPs in decentralized control manner as shown in the simulation results. Walking with precisely following the adequate trajectory and CPs, the robot will be capable to traverse versatile environments reliably and smoothly. The CPs which are contacted by the feet of head segment should be planned in each step by the head segment itself using the perception system. The integration of the walking control and planning both the CPs and the desired trajectory is one of our future works.

## 5. Conclusion

In this paper, a novel control method for a segmented multi-legged robot whose segment has a pair of 3-DoF legs and a 2-DoF active intersegment joint. The Follow-the-Contact-Point (FCP) gait control for the legs and the control of intersegment joints are consistently integrated thanks to introducing CP coordinate systems. The proposed control method was verified by a robot simulator, v-rep (Virtual-Robot Experimentation Platform), which showed that a multi-legged robot with 10 segments could walk on a curvilineal trajectory on flat terrain and traverse a stairs-like obstacle with maximum angle of $\pi/3$. Developing a real robot and implementing the proposed control method is one of our future works.

## Acknowledgements

This work was supported by JSPS KAKENHI Grant Number 25420217.

## References

[1] Yongchen Tang, Shugen Ma, Yi Sun, Dingxin Ge. Planar legged walking of a passive-spine hexapod robot. Advanced Robotics, **29**–23. 2015. p.1510–1525.

[2] Katie L. Hoffman, Robert J. Wood. Passive undulatory gaits enhance walking in a myriapod millirobot. Proc. of IEEE/RSJ Int. Conf. on Intelligent Robots and Systems. 2011. p.1479–1486.

[3] K.Tsuchiya, S.Aoi, and K.Tsujita. Locomotion control of a multi-legged locomotion robot using oscillators. SMC, 2002 IEEE Int. Conf. on, Vol.4. 2002.

[4] S.Aoi, H.Sasaki, and K.Tsuchiya. A multilegged modular robot that meanders: investigation of turning maneuvers using its inherent dynamic characteristics. SIAM Journal on Applied Dynamical Systems, 6-2. 2007. p.348-377.

[5] A.Torige, S.Yagi, H.Makino, T.Yagami, and N.Ishizawa. Centipede type walking robot. Proc. of IEEE/RSJ Int. Conf. on Intelligent Robots and Systems. 1997. p.402–407.

[6] Shinkichi Inagaki, Tomoya Niwa, Tatsuya Suzuki, T. Follow-the-Contact-Point gait control of centipede-like multi-legged robot to navigate and walk on uneven terrain. Proc. of IEEE/RSJ Int. Conf. on Intelligent Robots and Systems. 2010. p.5341–5346.
[7] Michael Sfakiotakis, D.P. Tsakiris, K.Karakasiliotis. Polychaete-like Pedundulatory Robotic Locomotion. Robotics and Automation, 2007 IEEE International Conference on. April 2007. p.269–274.
[8] L. Matthey, L. Righetti, and A.J. Ijspeert. Experimental study of limit cycle and chaotic controllers for the locomotion of centipede robots. Proc. of IEEE/RSJ Int. Conf. on Intelligent Robots and Systems. 2008 p.1860-1865.
[9] Geoffrey Long, Jay Anderson, and Johann Borenstein. The OmniPede: A New Approach to Obstacle Traversion. Proc. of IEEE International Conference on Robotics and Automation. 2002. p.714–719.
[10] Tianqi Wei, Qingsheng Luo, Yang Mo, Yong Wang, and Zhineng Cheng. Design of the three-bus control system utilising periodic relay for a centipede-like robot. Robotica, Available on CJO 2014 doi:10.1017/S0263574714002628
[11] F. Ozguner, S.J. Tsai, and R.B. McGhee. An Approach to the Use of Terrain- Preview Information in Rough-Terrain Locomotion by a Hexapod Walking Machine. The International Journal of Robotics Research, **3**–2. 1984. p.134–146
[12] M.D. Donner. Real-Time Control of Walking. Birkhauser Boston Inc. 1987.
[13] S.M. Song and B.S. Choi. A study on continuous follow-the-leader (FTL) gaits: an effective walking algorithm over rough terrain. Mathematical Biosciences, **97**–2. 1989. p.199–233.
[14] Marc D. Donner. Real-time control of walking. Birkhauser Boston Inc.; sec.2. 1987.
[15] Shundo Kishi and Shinkichi Inagaki. Graph-Search Based Footstep Planning for Multi-Legged Robots on Irregular Terrain by Using Depth-Sensor. 17th International Conference on Climbing and Walking Robots and the Support Technologies for Mobile Machines (CLAWAR 2014). 2014. p.417–424.
[16] Coppelia Robotics v-rep. www.coppeliarobotics.com/

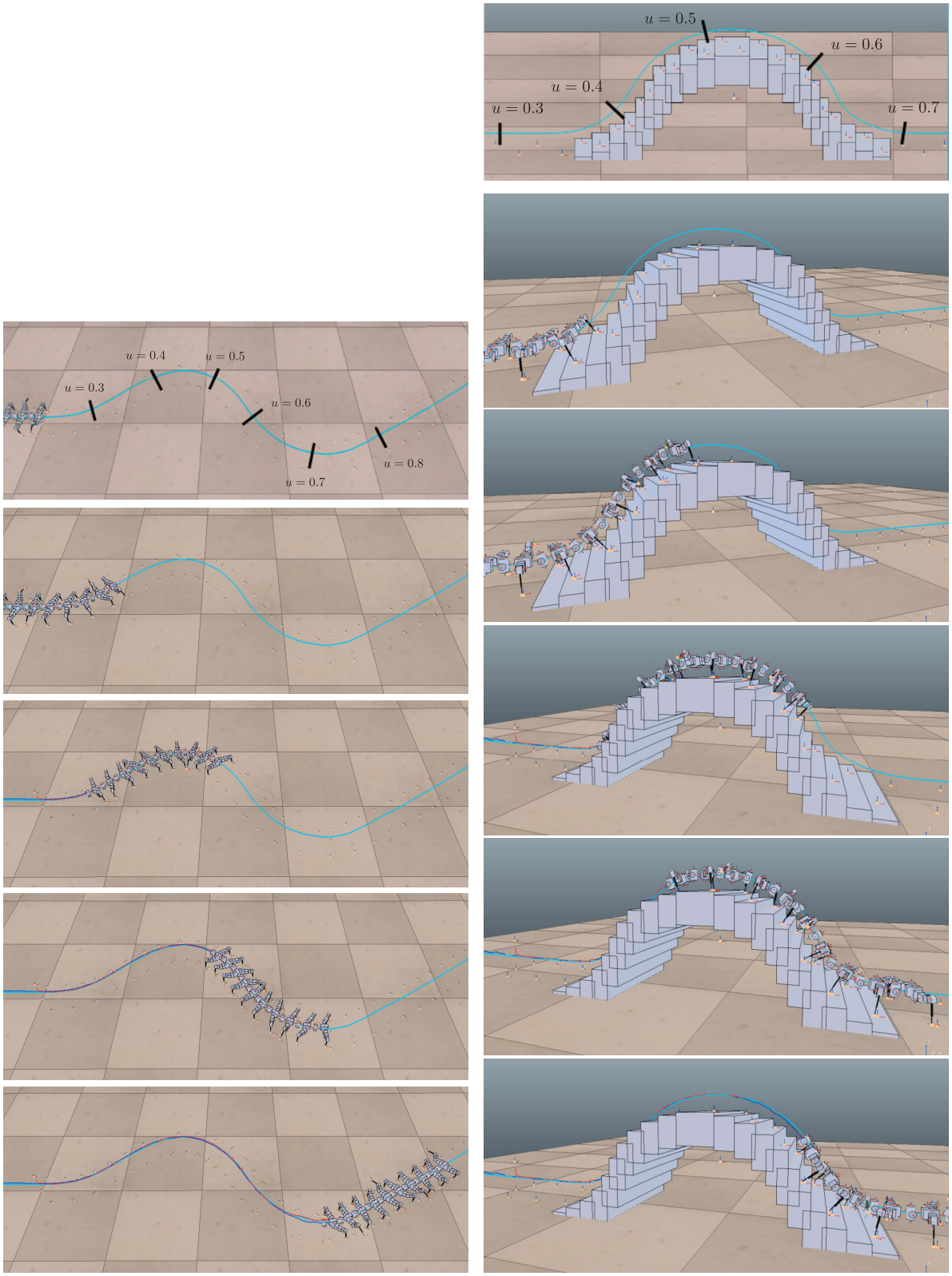


(a) Curvilineal trajectory on flat terrain.

(b) Stairs-like obstacle.

Figure 9. Simulation scenes of the segmented multi-legged robot walking on flat terrain and stairs-like obstacle with maximum angle of $\pi/3$

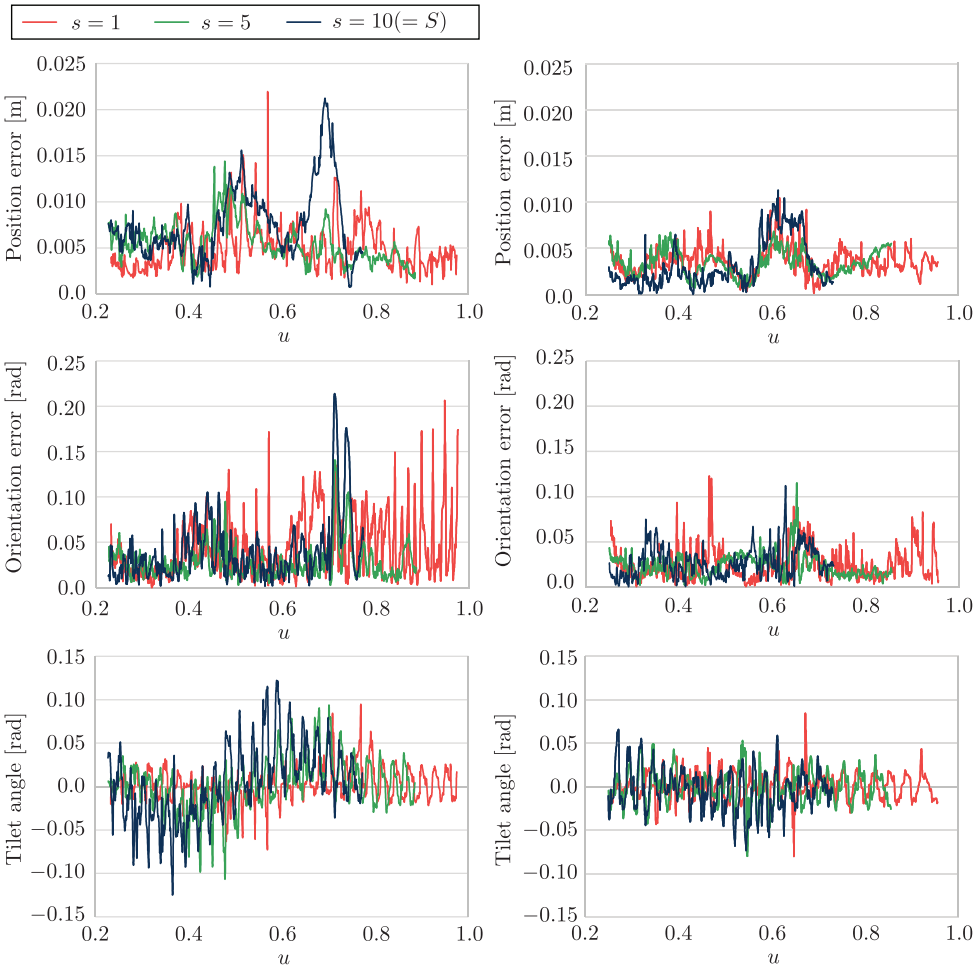


(a) Flat terrain (b) Stairs

Figure 10. Position and orientation errors of the body against the desired trajectory (upper and middle) and the tilt angle of each body (lower) : Walking curvilineal trajectory on flat terrain (a); and walking on stairs (b)